Computational Determination Of Binding Energy Of Ethane With [Mn(4-Picoline)₃]²⁺ Dication Complex Ion On DFT And PEC Models In The Gas Phase

Joseph K. Koka

School of Chemistry, University of Nottingham,
University Park, Nottingham, United Kingdom
School of Physical Science, Department of Chemistry,
University of Cape Coast, Ghana

Abstract: Stimulated by the quest for ways of a more resourceful convention of the abundant, untapped reserves of ethane, topical development in the gas-phase activation of ethane by metal dication complex ion [Mn(4-Picoline)3]2+ i.e [Mn(4-methyl Pyridine)3]2+ is discussed. The gas phase theoretical and experimental analysis on [Mn(4-Picoline)3]2+ was conducted. The ions were prepared using a combination of the pick-up technique and high energy electron impact, and then held in a cold ion trap where they were excited with tuneable UV radiation and further successfully activated with ethane

The average calculated binding energy per molecule of 4-Picoline (4-methyl Pyridine) calculated for [Mn(4-Picoline)3)2+,lied within the photon energy range over which the photofragmentation spectra were recorded. At the optimised geometry of [Mn(4-Picoline)3)2+ with ethane C1 symmetry was observed. The calculated DFT charge on the manganese metal centre in the optimised geometry was observed to be 20% lower than the potential energy curve (PEC) assumed charge of +2 on the manganese metal. The calculated binding energy of ethane with the Mn(4-Picoline)3]2+ was observed to be overestimated on the PEC by 24% as compare to the calculated DFT.

Keywords: Manganese, Binding energy, 4- Picoline, Potential energy curve, DFT, Gas Phase.

I. INTRODUCTION

Ethane is the second most significant hydrocarbon emitted to the atmosphere from oil and gas after methane [1] and is produced mainly via thermogenic processes [2]. A new study led by the University of Colorado Boulder stated that global emissions of ethane, an air pollutant and greenhouse gas, are on the uptick again. According to the study a steady decline of global ethane emissions following a peak in about 1970 ended between 2005 and 2010; in most of the Northern Hemisphere and has since reversed. Currently, research has shown that between 2009 and 2014, ethane emissions in the Northern Hemisphere increased by about 400,000 tons annually, the bulk of it is from North American oil and gas activity. Clearly, about 60 percent drop in the levels of ethane

over the past 40 years has already been made up within five years [3]. *Ethane pollution* can also harm agricultural crops [4]**.** Using ethanol fuel to power automobiles, results in significantly low levels of toxins in the environment [5]. Ethanol has a higher octane number than gasoline, providing premium blending properties. Minimum octane number requirements for gasoline prevent engine knocking and ensure drivability. Low-octane gasoline is blended with 10% ethanol to attain the standard 87 octane [6].

Over the past years the agenda for many governments, was emphasised on reducing fuel emissions. In an attempt to reduce their collective carbon footprint, many countries have started looking for a way to control their impact on the environment. This initiated a situation where the use of ethanol fuel has increased in many countries. Since the 1920s

the technology for creating ethanol fuel existed, but really took off in the 1980s, starting in Brazil. Looking for renewable, alternative fuel sources, the Brazilian government saw that around 90% of the country's cars ran on ethanol in the 80s and by 2012: approximately 87% of newly-registered vehicles run on ethanol and it has 16 million of the world's 27 million flexible fuel vehicles (FFVs) leading to 30% drop in petrol consumption in December 2011 [7]. To reduce air pollution more than 98% of U.S. gasoline contains ethanol, typically E10 (10% ethanol, 90% gasoline), to oxygenate the fuel. Ethanol which are used in FFVs is also available as E85 (or flex fuel), designed to operate on any blend of gasoline and ethanol up to 85%. Another blend, E15, was approved for use in model year 2001 and newer vehicles [8]. Currently, all new cars produced in Brazil have flexi-fuel engines which run on 100 per cent ethanol or 100 per cent petrol or any combination of the two. In addition, there is a 20 per cent mandatory ethanol addition to petrol [9]. The U.S. EPA in 2010 designated Brazilian sugarcane ethanol as an advanced biofuel due to its 61% reduction of total life cycle greenhouse gas emissions, including direct indirect land use change emissions [10,11]. In 2006, the government of India launched a programme of five per cent mandatory ethanol blending [12].

The advantages of ethanol compare to gasoline from the vehicle perspective are that ethanol has an antiknock ability, engine efficiency and torque output [13].

Research revealed that Audergon *et al* compared pyridine and 4-methyl-pyridine as ligands to cobalt (II) chloride in the gas phase and in solution [14], while Natalya *et al* in the gas-phase analysed the electron diffraction and quantum chemical calculations of the molecular structure of 4-methylpyridine-N-oxide [15]. The complexation of cobalt(II), nickel(II), and copper(II) ions with 4-methylpyridine (Picoline) in acetonitrile were also studied [16]. Further, the nature of the coordination bond in metal complexes of substituted pyridine derivatives. 111. 4-methylpyridine complexes of some divalent transition metal ions were studied [17]. In another development the detailed synthesis, spectroscopy, magnetic properties and crystal structure of four new Co(II) complexes with 2-amino-4-methylpyridine, 2-amino-3-methylpyridine, or 2-amino-5 chloropyridine were researched [18]. Hamish *et al* gave detailed experimental and theoretical study of the UV photofragmentation spectroscopy of the alkaline earth metal dications Mg^{2+}, Ca^{2+}, and Sr^{2+} complexed with pyridine and 4-methyl pyridine (4-picoline) [19].

Despite these successes literature review suggested no work was done on activation of ethane by $[Mn(4\text{-Picoline})_3]^{2+}$ ions in the gas phase. The primary aim of this research is to form doubly charged metal dication complexes $[Mn(4\text{-Picoline})_3]^{2+}$ ions, activate them with ethane in the gas phase and calculate the binding energy of ethane to the metal complexes. Once ethane is trapped from the atmosphere its activation can serve as feedstock formation in a vast variety of prominent industrial reactions in which, environmentally friendly chemical products formed have a significant impact on the climate due to the low-cost of this feedstock, on the chemical industry [20]. Envisage a chemical reactor that has atmospheric ethane as input where resources of ethane would be partially oxidised to ethanol according to Equation (1) be used much more efficiently. Ethanol as a liquid, easily

transportable, and chemically versatile product offers several advantages and it has even been suggested as the basis of future energy economy [21].

$$C_2H_6 + \frac{1}{2}O_2 \rightarrow C_2H_5OH \qquad \text{Equation} \quad 1$$

II. EXPERIMENTAL SECTION

$[Mn(4\text{-Picoline})_3]^{2+}$ ions were synthesised in the gas phase and their spectra recorded via UV photofragment spectroscopy within an ion trap mass spectrometer cooled to between 100-150K. A schematic diagram of the apparatus is shown in Figure 1. Neutral [Mn 4-Picoline]n clusters were generated via the pickup technique [22], whereby argon carrier gas at a pressure of 130 psi was passed through a reservoir of 4-Picoline held at room temperature. The resultant mixture, containing approximately 1% 4-Picoline vapour, underwent supersonic expansion through a 50mm diameter nozzle before passing through a 1 mm diameter skimmer. The emerging beam of mixed argon/4-Picoline clusters then passed over the top of a Knudsen cell containing manganese chips heated to $1150^{o}C$, which was sufficient to generate a metal vapour pressure of 10-3 to 10-2 mbar. Collisions between metal vapour and the mixed clusters generated neutral metal-containing clusters, which were then ionised by high energy electron impact (100 eV) in the ion source of a quadrupole mass spectrometer (Extrel). From the mixture a doubly charged ions, $[Mn(4\text{-Picoline})_3]^{2+}$ was mass selected and directed by an ion guide into a Paul ion trap.
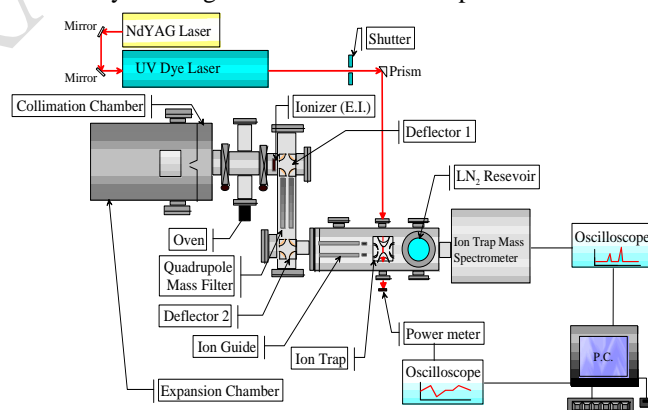
Figure 1: The diagram illustrating the experimental set up

The end caps of the latter were grounded and continuously cooled through direct contact with a liquid nitrogen reservoir. As a result, helium buffer gas ($5x10^{-4}$ mbar) contained within the trap was also cooled and over a total trapping time of 1s, collisions between the helium and trapped ions led to a considerable reduction in the internal energy content of the latter [23]. Based on the observation of unimolecular decay by trapped ions, the internal temperature was thought to drop from 4500 K to somewhere in the range 100–150 K. This cooling procedure has led to the appearance of discrete sharp mass spectrum of $[Mn(4\text{-Picoline})_3]^{2+}$ at 167 amu and a miniature hydrated complex of $[Mn(4\text{-Picoline})_3H_2O]^{2+}$ at 176 amu. (Figure 2).
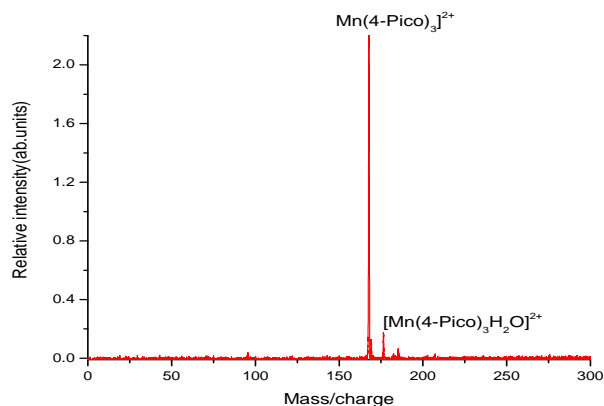
Figure 2: Mass spectrum of [Mn(4-Picoline)$_3$]$^{2+}$

With the introduction of ethane gas into the ion trap four additional peaks of the parent picking a molecule of ethane to form [Mn(4-Pico)$_3$C$_2$H$_6$]$^{2+}$ at 182 amu, a molecule of carbon dioxide to form Mn(4-Picoline)$_3$CO$_2$]$^{2+}$ at 189 amu, a molecule of water to form [Mn(4-Picoline)$_3$H$_2$O]$^{2+}$ at 176 amu, two molecules of water to form [Mn(4-Picoline)$_3$(H$_2$O)$_2$]$^{2+}$ 185 amu and the parent losing 4-Picoline molecule and 4-Picoline$^+$ to form [Mn4-Picoline]$^+$ at 148 amu Figure 3.

The spectra demonstrates the ability of the metal complex to fragment in the absence of laser radiation revealing that complexes under certain favourable conditions can dissociate by collision induced dissociation (CID) process. The carbon dioxide recorded in this spectrum was probably introduced into the ion trap from the ethane pipe line since no clear pronounced carbonated peak of [Mn(4-Pico)$_3$CO$_2$]$^{2+}$ was observed in Figure 2.
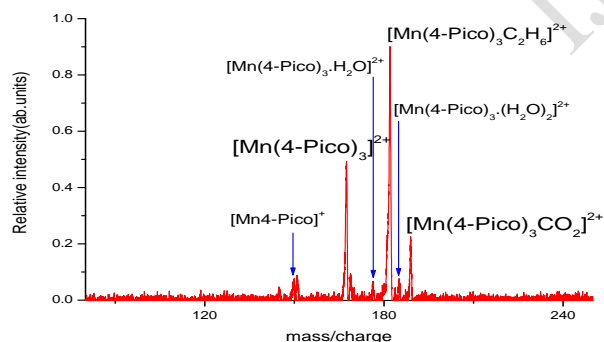
Figure 3: Fragmentation Mass spectrum of [Mn(4-Pico)$_3$C$_2$H$_6$]$^{2+}$ in the absence of laser irradiation

PHOTOFRAGMENTATION PATTERN OF [Mn(4-PICOLINE)$_3$C$_2$H$_6$)]$^{2+}$ COMPLEXES

A clear analysis of the photofragment mass spectra plotted from the average of the data generated over every 200 ion trap cycles when irradiated by laser revealed six distinct peaks as evidence in Figure 4. These are identified from a low consistent baseline but similar to fragments displayed in Figure 3 having a photofragmentation path with the loss of a molecule of 4-picoline and one molecule of 4-picoline ion resulting in the formation of a major daughter fragment peak corresponding to coordinately unsaturated [Mn4-Picoline]$^+$ at

148 amu. Figure 3 is clear evidence that under certain conditions manganese 4-picoline dication complex ions could collide and absorbed enough energy to dissociate similar to UV energy absorption photofragmentation Figure 4. However, under laser power the percentage ion peak intensities increase approximately 14times for Mn(4-Picoline)$_3$CO$_2$]$^{2+}$, [Mn(4-Picoline)$_3$(H$_2$O)$_2$]$^{2+}$ 4times, [Mn(4-Picoline)$_3$H$_2$O]$^{2+}$ 20 times while the parent fragment [Mn(4-Picoline)$_3$]$^{2+}$ 5time. Furthermore the fragment [Mn4-Picoline]$^+$ increase approximately 25times.
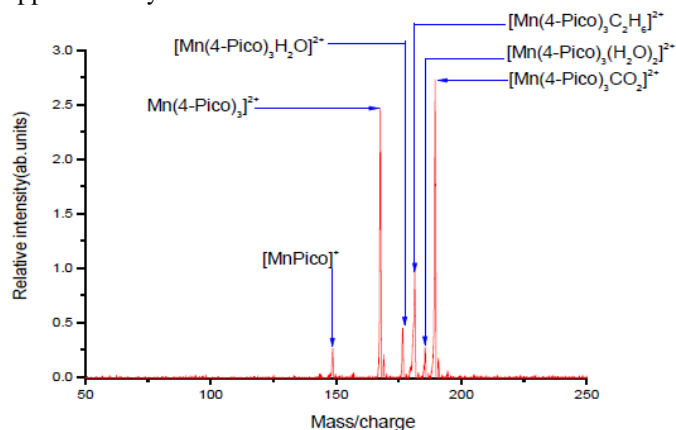
Figure 4: Photofragment mass spectrum of [Mn(4-Pico)$_3$Ethane]$^{2+}$ (Photon energy = 38095cm^{-1})

III. RESULTS AND DISCUSSION

Reaction	BVP86/kJ/mol	TPSSh/kJ/mol
[Mn(4-Picoline)$_3$]$^{2+}$ → Mn^{2+} + 3(4-Picoline)	1617.31	1617.31
Mn(4-Picoline)$_3$Et]$^{2+}$ → [Mn(4Picoline)$_3$]$^{2+}$ + Et	21.11	21.10

Table 1: Binding Energies for the [Mn(4-Pico)$_3$Ethane]$^{2+}$ Complexes with respect to various Products formed and Calculated using both BVP86/6311++G(d, p) and TPSSh/6311++G(d, p)

At the same levels of theory the calculated one-third the binding energy of the reaction [Mn(4-Picoline)$_3$)$^{2+}$ → Mn^{2+}+ 3(4-Picoline) at zero point energy corrections are in realistic agreement between BP86/6-311++G(d,p) and TPSSh/6-311++G(d,p) and equate to 539.10 kJ/mol (45065.2 cm^{-1}) per molecule which fall within the experimental photon energy range over which the photofragmentation spectra were recorded.

THE OPTIMISED GEOMETRY [Mn(4-PICOLINE)$_3$ C$_2$H$_6$]$^{2+}$

For the optimised structure of [Mn(4-Pico)$_3$C$_2$H$_6$]$^{2+}$ the shortest manganese-ethane (Mn-C) distance of 3.11 Å and the symmetry observed is C$_1$ (Figure 5).

*Figure 5: The optimized geometry of Mn(4-Pico)₃C₂H6]²⁺
with C1 Symmetry*

THE ONE DIMENTIONAL POTENTIAL ENERGY CURVE OF $[Mn(4-Picoline)_3C_2H6]^{2+}$

A one dimensional potential energy curve model is plotted (Figure 6) in order to picture the observed charge separation reaction qualitatively. The photo induced charge transfer to give $[Mn(4-Picoline)_3]^+$ and $C_2H_6^+$ of $Mn(4-Picoline)_3C_2H_6]^{2+}$ was not observed because this reaction is endothermic as evidenced by observing that the potential energy curve (black) lies above the attractive curve (red). At the optimised structure of $[Mn(4-Picoline)_3C_2H_6]^{2+}$ the shortest manganese-ethane (Mn-C) distance is 3.11 Å (Figure 7) which corresponds to approximately 0.27 eV (26.19 kJ/mol) as the binding energy from the PEC. The optimised geometry of $[Mn(4-Picoline)_3C_2H_6]^{2+}$ has C_1 symmetry. The calculated DFT binding energy of C_2H_6 to manganese 4-picoline dication complex ion is 21.11 kJ/mol resulting in the energy difference of 5.08 kJ/mol between the DFT and PEC calculations. This variance is due to difference in charge on the manganese metal while a calculated charge of Mn=1.62 was observed in the optimised geometry of $[Mn(4-Pico)_3C_2H_6]^{2+}$, Mn=2 was assumed in the PEC calculation.
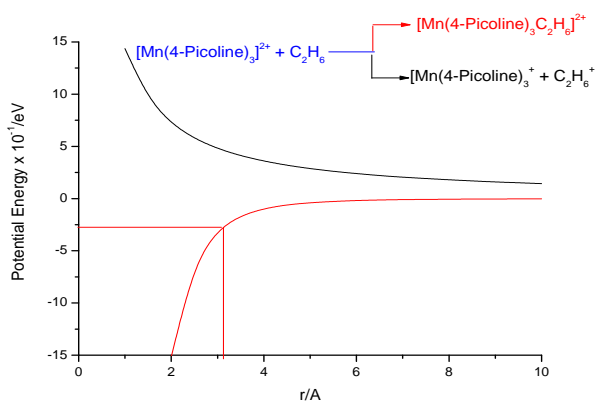
*Figure 7: Potential Energy Surface Curve model showing
attractive curve of ion-ligand $[Mn(4-Picoline)_3C_2H_6]^{2+}$*

IV. CONCLUSION

Ethane was successfully trapped and activated by $[Mn(4-Picoline)_3]^{2+}$, in the gas phase to form $[Mn(4-Picoline)_3C_2H_6]^{2+}$. The average binding energy per molecule of 4-Picoline calculated for $[Mn(4-Picoline)_3]^{2+}$, lied within the photon energy range over which the photofragmentation spectra were recorded. At the optimised geometry of $[Mn(4-Picoline)_3]^{2+}$ with ethane is C_1 symmetry was observed. The DFT calculated charge on the manganese metal centre of the optimised geometry was observed to be 20% lower than the PEC calculation. The calculated binding of ethane with the $Mn(4-Picoline)_3]^{2+}$ was observed to be overestimated on the PEC by 24% as compare to DFT calculation.

ACKNOWLEDGEMENT

REFERENCES

[1] https://www.sciencedaily.com/releases/2016/06/160614100242.htm Retrieved 2018-11-22.
[2] https://agupubs.onlinelibrary.wiley.com/doi/full/10.1029/2018JD028622 Retrieved 2018-11-22.
[3] https://www.eurekalert.org/pub_releases/2016-06/uoca-gec061316.php Retrieved 2018-11-22.
[4] Michael Biesecker, Matthew Brown; Associated Press Bakken oil field is causing a rise in air pollution, study. Apr 29, 2016. Retrieved 2018-11-22.
[5] https://www.conserve-energy-future.com/ethanol-fuel.php. Retrieved 2018-11-2.
[6] https://afdc.energy.gov/fuels/ethanol_fuel_basics.html Retrieved 2018-11-22.
[7] https://www.arnoldclark.com/newsroom/347-can-cars-run-on-alcohol Retrieved 2018-11-22.
[8] https://www.thehindu.com/opinion/op-ed/a-sugar-rush-that-could-fuel-the-economy/article5160989.ece. Retrieved 2018-11-22.
[9] Flexible Fuel Vehicles: Providing a Renewable Fuel Choice (Fact Sheet)" (PDF). U.S. Department of Energy. June 2008. Retrieved 2018-12-22
[10] Greenhouse Gas Reduction Thresholds". U.S. Environmental Protection Agency. 2010-02-03. Retrieved 2018-12-01.
[11] "EPA designates sugarcane ethanol as advanced biofuel". Green Momentum. 2010-02-05. Archived from the original on July 11, 2011. Retrieved 2018-12-01.
[12] file:///G:/Ethanol/A%20sugar%20rush%20that%20could%20fuel%20the%20economy%20%20Ethane.htm. Retrieved 2018-12-01.

[13] Author links open overlay panel JianlingJiao Jingjing, LiYuBai Journal of Cleaner Production Volume 180, 10 April 2018, 832-845 Retrieved 2018-11-22.

[14] L. Audergon, M.Piccand, F. Emmenegger, H. Piekarski (2001) Comparison of pyridine and 4-methyl-pyridine as ligands to cobalt(II) chloride in the gas phase and in solution 20(5):387-394. DOI: 10.1016/S0277-5387(00)00635-5

[15] Natalya V. Belova, Vitaliya E. Kotova, Georgiy V. Girichev, Kseniya A. Korolkova (2017) The molecular structure of 4-methylpyridine-N-oxide: Gas-phase electron diffraction and quantum chemical calculations J. of Molecular Structure 1156 DOI: 10.1016/j.molstruc.2017.11.070.

[16] Makoto Kurihara, Takuji Kawashima, and Kazuhiko Ozutsumi (2000) Complexation of Cobalt(II), Nickel(II), and Copper(II) Ions with Pyridine, 2-Methylpyridine, 3-Methylpyridine, and 4-Methylpyridine in Acetonitrile. erlag der Zeitschrift für Naturforschung, Tübingen • www.znaturforsch.com

[17] D. G. Brewer, P. T. T. Wong, M. C. Sear (1968) The nature of the coordination bond in metal complexes of substituted pyridine derivatives. 111. 4-Methylpyridine complexes of some divalent transition metal ions

[18] Raziyeh Arab Ahmadi, Hamid Reza Khavasi, Nasser Safari, Saeid Amani (2011) Four new Co(II) complexes with 2-amino-4-methylpyridine, 2-amino-3-methylpyridine, or 2-amino-5-chloropyridine: Synthesis, spectroscopy, magnetic properties, and crystal structure Journal of Coordination Chemistry 64(12):2056-2065 DOI: 10.1080/00958972.2011.587877.

[19] Hamish Stewart, Guohua Wu, Lifu Ma, Michael Barclay, Andreia Dias Vieira, Andrew King, Hazel Cox, Anthony J. Stace (2011) Ultraviolet Photofragmentation Spectroscopy of Alkaline Earth Dication Complexes with Pyridine and 4-Picoline (4-Methyl pyridine). J. Phys. Chem. A, 115 (25), pp 6948–6960 DOI: 10.1021/jp112171j

[20] F. ViÇes, Y. Lykhach, T. Staudt, M. P. A. Lorenz, C. Papp, Hans-Peter Steinruck, J. Libuda, K. M. Neyman, A. Gorling (2010) Methane Activation by Platinum: Critical Role of Edge and Corner Sites of Metal Nanoparticles Chem. Eur. J. 16, 6530 – 6539 DOI: 10.1002/chem.201000296

[21] A.V. Bridgwater (2007) The production of biofuels and renewable chemicals by fast pyrolysis of biomass Int. J. Global Energy Issues, 27(2):160-203 •DOI: 10.1504/IJGEI.2007.013654 •

[22] A.J. Stace, (2002) Metal Ion Solvation in the Gas Phase: The Quest for Higher Oxidation States J. Phys. Chem. A 106, 7993 DOI: 10.1021/jp020694t

[23] G. Wu, D. Chapman and A.J. Stace,(2007). Trapping and recording the collision- and photo-induced fragmentation patterns of multiply charged metal complexes in the gas phase Int. J. Mass Spectrom.262, 211 262: 211-219. DOI: 10.1016/j.ijms.2006.11.012